Available online at www.sciencedirect.com
ScienceDirect
Journal of Photochemistry and Photobiology A: Chemistry 184 (2006) 177–183
Journal of Photochemistry and Photobiology A:Chemistry
www.elsevier.com/locate/jphotochem

One- and two-photon photochromism of 3,4-bis-(2,4,5-trimethyl-thiophen-3-yl)furan-2,5-dione

Claudia C. Corredor[a,c], Kevin D. Belfield[a,*], Mykhailo V. Bondar[b], Olga V. Przhonska[b], Florencio E. Hernandez[a], Oleksiy D. Kachkovsky[d]

[a] *Department of Chemistry and College of Optics and Photonics: CREOL and FPCE, University of Central Florida, P.O. Box 162366, Orlando, FL 32816-2366, United States*
[b] *Institute of Physics, Prospect Nauki, 46, Kiev-28, 03028 Kiev, Ukraine*
[c] *Bristol-Myers Squibb Pharmaceutical Research Institute, One Squibb Drive, P.O. Box 191 New Brunswick, NJ 08903-019, United States*
[d] *Insitute of Organic Chemistry, Murmanskaya Street, 5, Kiev 03094, Ukraine*

Received 31 January 2006; received in revised form 7 April 2006; accepted 10 April 2006
Available online 28 April 2006

Abstract

Photochromic properties of the diarylethene derivative 3,4-bis-(2,4,5-trimethyl-thiophen-3-yl)furan-2,5-dione (**1**) were investigated in hexane at room temperature under one-photon (linear) and two-photon (nonlinear) excitation. Results of steady-state excitation anisotropy and quantum–chemical calculations (AM1, ZINDO/S) provide insight into the nature of the broad absorption spectrum of the open-form of **1** as an overlapped mixture of several electronic transitions. The quantum yields of cyclization and cycloreversion reactions of **1** were obtained over a broad spectral range and the photochemical stability of **1** was determined for different excitation wavelengths. The two-photon absorption (2PA) spectrum of the open-form of **1**, with maximum cross-section ≈80 GM at 674 nm, was obtained using an up-converted fluorescence method. Two-photon induced cyclization reaction of **1** was accomplished under picosecond excitation and the corresponding reaction quantum yield was estimated, providing a comprehensive investigation of this 2PA photochrome.

Keywords: Photochromic; Photoisomerization; Diarylethene; Two-photon excitation

1. Introduction

Photochromic properties of organic molecules have attracted scientific interest due to their potential application in the development of optical data storage materials [1–4]. Hirshberg constituted a chemical memory model based on a reversible change in the molecular structure during light irradiation [5]. Since that time a vast number of studies on photochromic properties of organic compounds were reported, including photoinduced *trans–cis* isomerization [6], valence tautomerism [7], homolytic cleavage [8], hydrogen transfer [9] and cyclization of π-conjugated chromophores [10]. In spite of multiple studies, organic photochromic compounds have found little application in optical data storage due to serious problems with their thermal and photochemical stability. Among the wide variety of photochromic molecules (see, for example, spiropyrans and spirooxazines [11], fulgides [12], azobenzenes [13], etc.); diarylethene derivatives are, perhaps, the most promising photochromic systems. They were developed by Irie et al. [14,15] and Lehn and co-workers [16,17] for application in high density optical memory devices.

Diarylethenes are a relatively new class of thermally irreversible photochromic compounds with excellent thermal stability, resistance to fatigue during cyclic write and erase processes, fast response, high sensitivity and nondestructive readout capability [18–21]. One of the most studied diarylethene compounds is 3,4-bis-(2,4,5-trimethyl-thiophen-3-yl)furan-2,5-dione (**1**) [14,18–20,22–25] The open-ring form (O) of **1** (Fig. 1) is transparent in the visible spectral range and undergoes cyclization reaction under UV irradiation resulting in the formation of the colored closed-ring form (C) [14]. The cycloreversion reaction C → O proceeds under visible and UV

* Corresponding author. Tel.: +1 407 823 1028.
E-mail address: kbelfiel@mail.ucf.edu (K.D. Belfield).

1010-6030/$ – see front matter © 2006 Elsevier B.V. All rights reserved.
doi:10.1016/j.jphotochem.2006.04.012

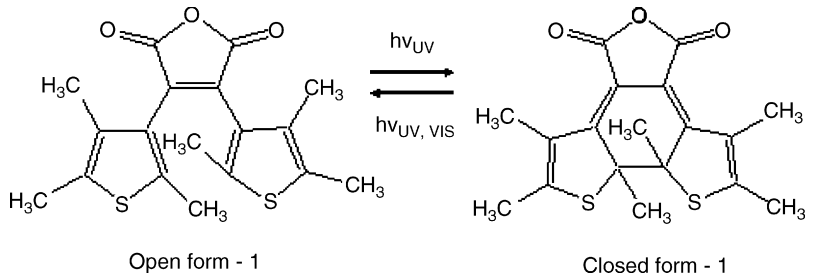

Fig. 1. Schematic diagram of the cyclization and cycloreversion photochromic (isomerization) reactions of **1**.

light irradiation resulting in the bleached open-ring form. The reversible photocyclization of **1** with more than 100 coloring and bleaching cycles under one-photon excitation has been reported [14]. Solvent effects on the photochromic reaction quantum yields along with the fluorescence properties of **1** were also investigated [22–25]. These measurements revealed at least two types of conformers in the excited state of diarylethene **1**. One of them is more planar conformer with C_2 symmetry (so-called "antiparallel" (AP)) which undergoes ring-closed processes, whereas another one is a twisted conformer with S_2 symmetry (so-called "parallel" (P)) which possesses intramolecular charge transfer character and exhibits no photochromic transformation [22,23]. Theoretical study by semi-empirical molecular orbital methods revealed several similar types of conformers which can exist in the ground state of **1**, and only AP conformers undergo photochemical reaction [18]. As assumed by Irie and co-workers [22,23], the relative amount of P and AP conformers in the ground state depends on solvent polarity, with less polar solvents corresponding to an increased amount of AP conformer.

The direct observation of the photochromic transformation of **1** under one-photon excitation was reported [20], where the time constants of the ring-closure, O → C and ring-opening, C → O processes were determined by a picosecond transient absorption spectroscopy method as <10 ps. However, little is known about two-photon photochromic properties of diarylethene derivatives due to their relatively low two-photon absorption (2PA) cross-sections. Experimental evidence of two-photon isomerization and orientation of 1,2-dicyano-1,2-bis-(2,4,5-trimethyl-3-thienyl)ethane in poly(methyl methacrylate) films was reported by Sekkat et al. [26]. The same dye-doped photochromic medium was investigated under two-photon excitation by Toriumi et al. [27,28] for the development of reflection confocal microscopy readout system for 3D optical memory. To our knowledge, no data have been reported on two-photon photochromic properties of **1**. This molecule is a promising photochromic compound for 3D-data storage technologies and its photophysical and photochemical properties exhibited under one- and two-photon excitation are a subject of great scientific interest and practical utility.

In this study, we report precise measurements of the photochromic and photochemical quantum yields of **1** over a broad spectral region, along with the two-photon absorption spectrum and experimental evidence of two-photon induced photocyclization. In addition, we report the results of quantum–chemical and kinetic processes calculations of the electronic model of **1** based on reports by Irie and co-workers [20,22]. The main goal of this paper is to provide a deeper understanding of the photochromic and photodecomposition processes in **1** under one- and two-photon excitation in order to provide the basis to develop a high quality 3D-data storage materials and optimize their write–read conditions.

2. Experimental

3,4-Bis-(2,4,5-trimethyl-thiophen-3-yl)furan-2,5-dione (**1**) was purchased from TCI America and used without further purification. Spectroscopic grade hexane (Alfa Aesar) was used as a solvent. The absorption spectra of the O-form and mixtures of O–C-forms of **1** were recorded with an UV–vis Agilent 8453 spectrophotometer. The pure C-form was separated from a mixture of open and closed forms in the photostationary state by normal phase HPLC, using a Waters HPLC instrument equipped with a binary pump (1525), an in-line degasser, a PDA detector (2996) and a manual injector (7725I). The best chromatographic separation was achieved by using a silica gel (4.6 mm × 150 mm, particle size 5 μm, pore size 100 Å) analytical column, with a mobile phase of 97:3, hexanes:ethyl acetate under isocratic flow. The flow was 0.5 mL/min, the injection volume was 50 μL, the column temperature was 30 °C and the run time was 10 min. Steady-state fluorescence and excitation anisotropy spectra were measured with a PTI Quantamaster spectrofluorimeter in the photon-counting regime of the PMT using an L-format configuration [29]. All fluorescence measurements were performed in 10 mm fluorometric quartz cuvettes for the concentrations, $C \leq 5 \times 10^{-6}$ M. The fluorescence quantum yield of **1**, $\Phi_{FL} \approx 0.003$, was determined by a standard method, relative to 9,10-diphenylanthracene in cyclohexane [29], corresponding well with data reported in ref. [24]. The concentration dependence of Φ_{FL} in hexane was estimated by the excitation of **1** at the appropriate wavelength, λ_{exc}, where optical density $D(\lambda_{exc}) \leq 0.1$. This dependence exhibited a nearly constant value of Φ_{FL} up to $C = 5 \times 10^{-4}$ M, and was used for the determination of 2PA cross-sections by the up-converted fluorescence method [30].

The quantum yields of the direct, $\Phi_{O\rightarrow C}$, and reverse, $\Phi_{C\rightarrow O}$, photochromic reactions (O → C and C → O reactions, respectively), were determined from the temporal changes in the corresponding absorption spectra of **1** under steady-state Xe-lamp irradiation passed through the excitation monochromator of the PTI Quantamaster spectrofluorimeter. All measurements were

performed at room temperature in the darkness because of the high sensitivity of **1** to ambient light. The values of $\Phi_{O\rightarrow C}$ and $\Phi_{C\rightarrow O}$ were obtained by the absorption method described in ref. [31] for air-saturated and degassed solutions prepared by repeated freeze–pump–thaw cycles. Briefly, this absorption method is based on measurement of the temporal changes in the optical density, D (λ, t) at $\lambda_{max} \approx 553$ nm (long wavelength maximum of the C-form of **1** in hexane), and optical density at the excitation wavelength, D (λ_{exc}, t), during irradiation. The O-form of **1** has no absorption at 553 nm and, thus, it is straightforward to determine the number of reacted molecules, whereas the number of absorbed photons by the O-form (for $\Phi_{O\rightarrow C}$) or C-form (for $\Phi_{C\rightarrow O}$) at λ_{exc}, was recalculated from the dependences D (λ_{exc}, t), taking into account the individual spectral shapes of the corresponding forms of **1**. Two milliliter hexane solutions of **1** with concentrations, $C \sim (1.5–2) \times 10^{-5}$ M, were placed into a 10 mm × 10 mm × 35 mm quartz cuvette and carefully sealed to avoid solvent evaporation during experiments. The entire volume of the solution was irradiated with light irradiance 0.05–0.3 mW/cm^2 in the 270–610 nm spectral range. The irradiation power was measured with a Laserstar power meter (Ophir Optronics Inc.) with the sensitivity in the nW range. The changes in the absorption spectra during irradiation were measured with an UV–vis Agilent 8453 spectrophotometer. A probe beam in this spectrophotometer was attenuated over 10-fold by neutral filters in order to reduce photocyclization process during the measurements. The same method was used for the determination of the photodecomposition quantum yields, Φ_{Ph}, of **1** under one-photon excitation. First, an equilibrium between two forms was reached at the corresponding λ_{exc}, and then the values of Φ_{Ph} were determined from the temporal changes in equilibrium spectra during the irradiation over a longer period of time.

The 2PA spectrum of the O-form of **1** was measured by the up-converted fluorescence method [30] using a femtosecond laser system (Clark-MXR 2010 Ti:Sapphire amplified, second harmonic of an erbium-doped fiber ring oscillator system (output 775 nm) pumped an optical parametric generator/amplifiers (TOPAS, Light Conversion), with pulse duration, $\tau_P \approx 140$ fs (FWHM), 1 kHz repetition rate, tuning range 560–2100 nm and maximum average power ≈ 25 mW). The up-converted fluorescence of the O-form of **1** was detected for solutions in 10 mm quartz cuvettes ($C \approx 4.4 \times 10^{-4}$ M) with a PTI Quantamaster spectrofluorimeter in the analog regime of PMT, relative to the fluorescein in water (pH 11) [30]. In order to decrease reabsorption effects, the laser beam excited solutions near the exit surface of the cuvette from which fluorescence was observed. The number of reacted molecules during these measurements was negligible.

The two-photon induced cyclization reaction of **1** was observed under high intensity excitation with a picosecond Nd:YAG laser (PL 2143 B Ekspla) coupled to an optical parametric generator (OPG 401/SH) with pulse duration, $\tau_P \approx 35$ ps (FWHM), pulse energy, $E_P \leq 100$ μJ, at the wavelength, $\lambda_{exc} = 810$ nm and repetition rate, $f = 10$ Hz. The excitation laser beam was focused into a 1 mm quartz cell of hexane solutions of **1** (the volume of solution was ∼40 μL; $C \sim 4.3 \times 10^{-3}$ M) to a waist of radius ∼0.12 mm. Appearance of the C-form of **1** was detected spectrophotometrically at $\lambda_{max} = 553$ nm.

Quantum–chemical calculations of the electronic structure of **1** were performed using HyperChem V 7.0 for Windows. The optimized geometry of **1** in the ground state was obtained via AM1 approximation. A semi-empirical ZINDO/S method, with the highest 10 occupied molecular orbitals (HOMO) and the lowest 10 unoccupied molecular orbitals (LUMO), was applied to determine the corresponding electronic spectra. Average overlap weighting factors of 1.267 were used for σ bonds, and the values of π weighting factors were chosen in the range 0.53–0.55 to obtain the best agreement with the long wavelength experimental maxima of the O- and C-forms absorption spectra of **1**.

3. Results and discussion

3.1. Steady-state spectral properties

The photoisomerization processes investigated for **1** are shown in Fig. 1.

Individual absorption spectra of the O- and C-forms of **1** in hexane are shown in Fig. 2, curves 1 and 2. Corresponding extinction coefficients of the O- and C-forms at λ_{max} were 7.2×10^3 M^{-1} cm^{-1} (331 nm) and 2.7×10^4 M^{-1} cm^{-1} (377 nm), respectively. The nature of the broad O-form absorption spectrum of **1** (Fig. 2, curve 1) was analyzed by excitation anisotropy and quantum–chemical calculations (Table 1). The excitation anisotropy spectrum of **1** in silicon oil is shown in Fig. 2, curve 5. In viscous silicon oil at room temperature, no fast rotation of **1**, and corresponding depolarization effects, occurs during the fluorescence lifetime ($\tau_{FL} \approx 360$ ps) [20,22], and excitation anisotropy, r, reaches its maximum value [29]:

$$r = \frac{(3\cos^2\alpha - 1)}{5}$$

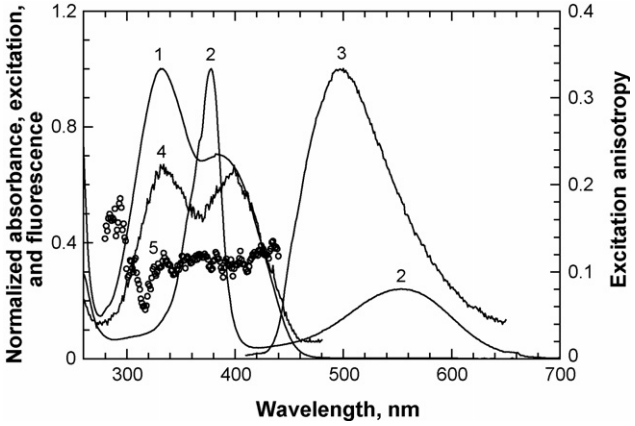

Fig. 2. Normalized absorption (1 and 2), corrected excitation (4) and fluorescence (3) and excitation anisotropy (5) spectra of the O-form (1 and 3–5) and C-form (2) of **1** in hexane. $\lambda_{obs} = 490$ nm is the wavelength of the observation of the excitation and anisotropy spectra (4 and 5). Excitation spectrum (4) is normalized to the absorption spectrum (1) at 400 nm.

Table 1
Calculated maximum wavelength, λ_{max}; oscillator strength, f; angle, β, relative to the orientation of $S_0 \rightarrow S_1$ transition; main orbital configuration (promotion of an electron from the HOMO to the LUMO, $|H \rightarrow L\rangle$, HOMO-1 to the LUMO, $|H\text{-}1 \rightarrow L\rangle$, and HOMO-2 to the LUMO, $|H\text{-}2 \rightarrow L\rangle$) for the first three π–π^* electronic transitions of the O-form AP conformer of **1**

Transition	λ_{max} (nm)	F	β (°)	Contribution to the main configuration
$S_0 \rightarrow S_1$	430	0.095	–	$0.97\|H \rightarrow L\rangle$
$S_0 \rightarrow S_2$	401	0.0285	90	$0.908\|H\text{-}1 \rightarrow L\rangle$
$S_0 \rightarrow S_3$	294	0.35	26	$0.94\|H\text{-}2 \rightarrow L\rangle$

where α is the angle between absorption, $S_0 \rightarrow S_n$, and emission, $S_1 \rightarrow S_0$, transition dipoles (S_0, S_1, S_n are the ground, first excited and higher excited electronic states, respectively). Changes in r at $\lambda < 320$ nm (Fig. 2, curve 5) reveal the spectral position of the different electronic states in the broad absorption spectrum of the O-form. In the spectral range $\lambda > 300$ nm the values of r did not exceed 0.14. Relatively low values of r at the long wavelength edge of the absorption band (Fig. 2, curve 1) may be explained by assuming strong overlap of several nonparallel absorption electronic transitions. This assumption was confirmed by the results of quantum–chemical calculations (Table 1). As can be seen, diarylethene **1** possesses of three nonparallel π–π^* absorption electronic transitions (with different angles, β, relative to the orientation of $S_0 \rightarrow S_1$ transition) in the 290–440 nm spectral range. A sufficiently large value of β (90°) between the $S_0 \rightarrow S_1$ and $S_0 \rightarrow S_2$ transitions, may be a reason for the reduction in anisotropy, even in the case when $\alpha = 0°$ [32]. High molecular symmetry as a contributing reason for the reduced anisotropy in the long wavelength absorption band [32], is less probable, because the symmetry of the reactable O-form (antiparallel) conformer of **1** is not very high (C_2 symmetry).

The excitation spectrum of the O-form (Fig. 2, curve 4) did not coincide with corresponding absorption curve 1, which indicated a decrease in the fluorescence quantum yield, Φ_{FL}, in the short wavelength part of the absorption spectrum, confirming a complicated electronic structure of the absorption band of the O-form.

3.2. Quantum yields of the photochromic reactions under one-photon excitation

The kinetic changes in the absorption spectra of **1** (hexane solutions) under the steady-state irradiation at $\lambda_{exc} = 330$ and 550 nm are shown in Figs. 3 and 4, respectively. Observed isobestic points of the absorption spectral changes reveal no photochemical products that can arise during the irradiation and affect the photoisomerization kinetics. The initial slopes of the dependences $N_{mol} = f(N_{ph})$ (where N_{mol} and N_{ph} are the number of reacted molecules and the number of absorbed photons, respectively) are shown in the insets of Fig. 3. These measurements were performed for different λ_{exc} in the absorption band of **1**, and the spectral dependences of the cyclization and cycloreversion reaction quantum yields were obtained (Fig. 4). From these data, a weak spectral dependence of $\Phi_{O\rightarrow C}$ and $\Phi_{C\rightarrow O}$ was observed. The values of $\Phi_{O\rightarrow C}$ were in the range 0.2–0.35 and differed by ca. a factor of two from previously reported data ($\Phi_{O\rightarrow C} \approx 0.13$) [23]. The cycloreversion quantum yields of **1**, $\Phi_{C\rightarrow O} \approx 0.1$–16, were in a good agreement with previously reported data [22,23].

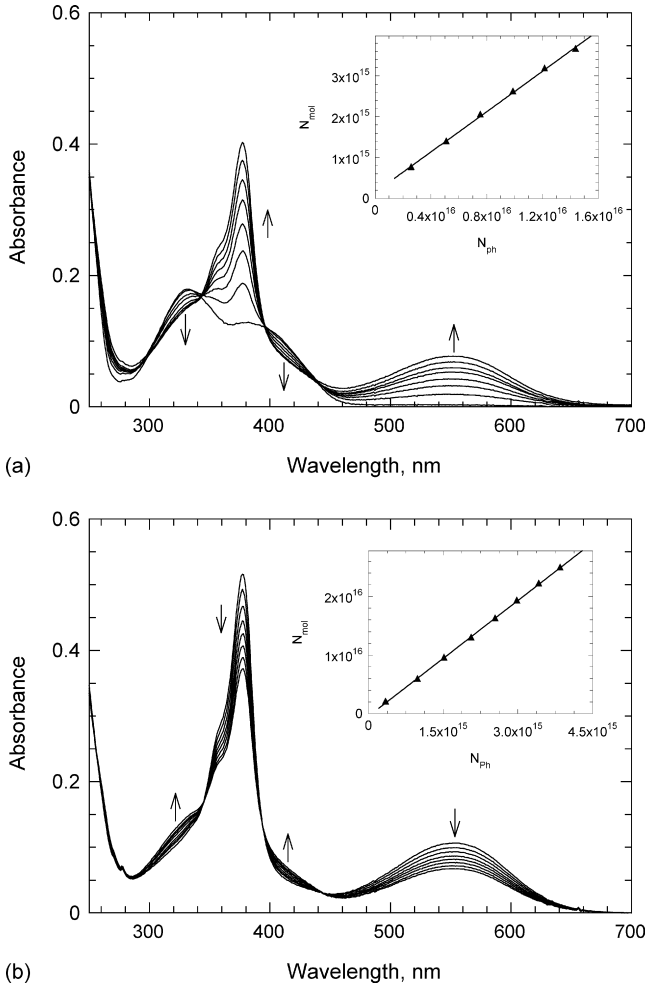

Fig. 3. Kinetic changes in the absorption spectra of **1** in hexane ($C \approx 2.5 \times 10^{-5}$ M) under irradiation at: (a) $\lambda_{exc} = 330$ nm and (b) $\lambda_{exc} = 550$ nm (temporal step between two adjacent spectra, $\Delta t = 100$ s, irradiance of the excitation ≈0.140 mW/cm^2 (a) and ≈0.100 mW/cm^2 (b)). The initial spectrum is an original O-form absorption (a) and photostationary state under the irradiation at $\lambda_{exc} = 415$ nm.

Air-saturated and deoxygenated hexane solutions of **1** exhibited nearly the same reaction efficiencies for both forms. This suggests that molecular oxygen has no falcon the fast picosecond photoisomerization processes of **1**.

A simplified electronic model of **1** (Fig. 5) is proposed on the basis of spectral properties (Fig. 2), on the results of quantum–chemical calculations, and also on the experimental and theoretical data reported by Irie et al. [14,20,22,23]. A distinctive feature of the photochromic transformations of **1** is a fast rate of the cyclization and cycloreversion processes: $\{1/k_{32}, 1/k_{31}\} \leq 10$ ps; $1/k_{10} \leq 2$–3 ps, demonstrated via picosecond transient absorption spectroscopy [20]. Examination of the spectral dependence (Fig. 4a), an increase in the value of $\Phi_{O\rightarrow C}$ at $\lambda_{exc} = 440$ nm reveals an efficient cyclization reaction

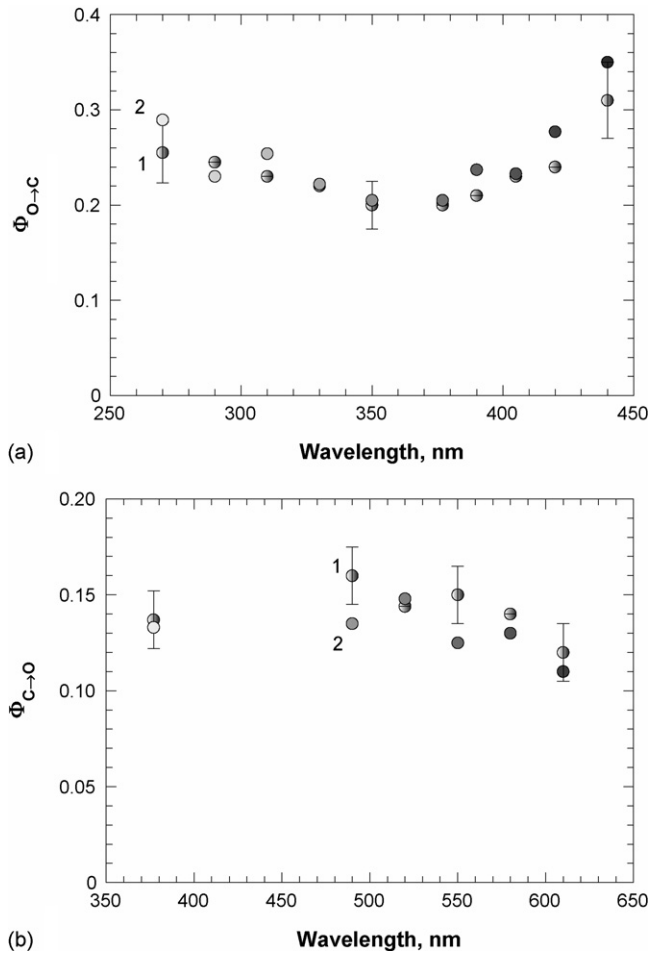

Fig. 4. Spectral dependences of the photocyclization, $\Phi_{O\rightarrow C}$ (a) and cycloreversion, $\Phi_{C\rightarrow O}$ (b), reaction quantum yields of **1** for air-saturated (1) and deoxygenated (2) hexane solutions.

$O \rightarrow C$ from the fluorescent state of the O-form with lifetime, $\tau_{FL} \approx 360$ ps. This is consistent with the results of transient absorption measurements of **1** in hexane [22]. Nearly the same values of $\Phi_{C\rightarrow O}$ at $\lambda_{exc} = 377$ and 550 nm (Fig. 4b) indicate the cycloreversion processes occurring at these wavelengths

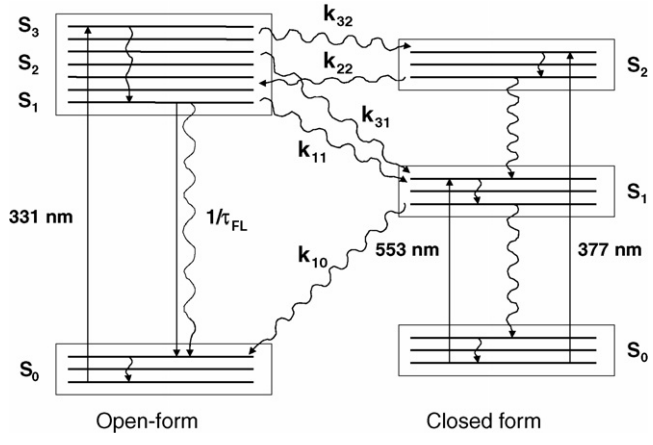

Fig. 5. Schematic representation of the electronic structures of the open and closed forms of **1**.

are similar in nature. This suggest that probable reaction pathway through the S_1 state of C-form (i.e. S_0 state of the C-form was excited to the S_2 state, then relaxed to the S_1 state and transformed to the S_0 state of the O-form with the corresponding velocity constant, k_{10} (Fig. 5) proceeds, instead of possible direct transformation $C \rightarrow O$ from the S_2 state with velocity constant k_{22}.

3.3. Kinetic analysis

The kinetics of the photochromic transformations of **1** under steady-state irradiation was calculated for different λ_{exc} in order to determine the optimized writing conditions for possible data recording. These calculations were performed with the differential equation:

$$\frac{dN_{CF}(t)}{dt} = -\sigma_{CF} \cdot I_0 \cdot N_{CF}(t) \cdot \Phi_{C\rightarrow O} + \sigma_{OF} \cdot I_0 \cdot N_{OF}(t) \cdot \Phi_{O\rightarrow C}, \quad (1)$$

where $N_{OF}(t)$, $N_{CF}(t)$, σ_{OF} and σ_{CF} are the concentrations and one-photon absorption cross-sections of the O- and C-forms, respectively and I_0 is the irradiance of the excitation light (in photon/(cm^2 s)).

Eq. (1) was solved numerically using the constant field approximation (i.e. $I_0 \approx$ constant in the entire irradiation volume), and with the start conditions: $N_{CF}(0) = 0$, $N_{OF}(0) = N_0$ (where $N_0 = N_{CF}(t) + N_{OF}(t)$ is the total molecular concentration of **1**, assumed to be constant). The concentration of the incipient C-form was calculated over a broad spectral range for various steady-state irradiation conditions. These calculations were based on known photophysical parameters of **1** and the observed spectral dependence of $\Phi_{O\rightarrow C}$ (the average value of $\Phi_{C\rightarrow O} \approx 0.14$, was considered constant over the entire spectral range). The spectral curves of the normalized values, N_{mol}/N_0 are shown in Fig. 6. λ_{exc} ≈330 and ≈400–405 nm, were found to be

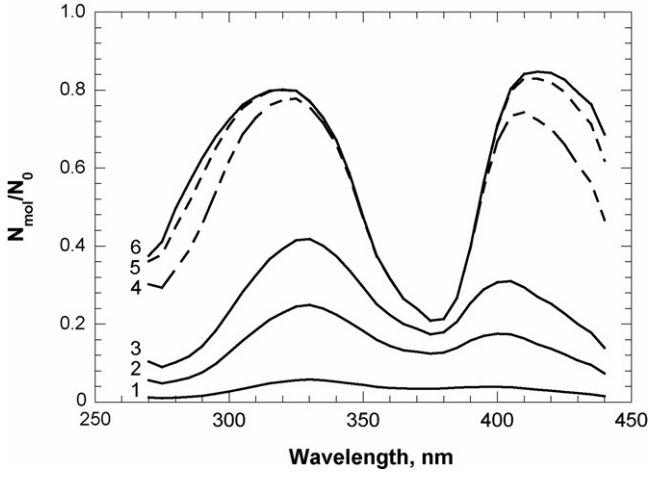

Fig. 6. Calculated spectral dependencies of the normalized concentration of the C-form of **1**, N_{mol}/N_0, forming with total irradiation dose (1) $F = 1 \times 10^{16}$ photon cm^{-2}, (2) 5×10^{16} photon cm^{-2}, (3) 1×10^{17} photon cm^{-2}, (4) 5×10^{17} photon cm^{-2}, (5) 1×10^{18} photon cm^{-2} and (6) 2×10^{18} photon cm^{-2}.

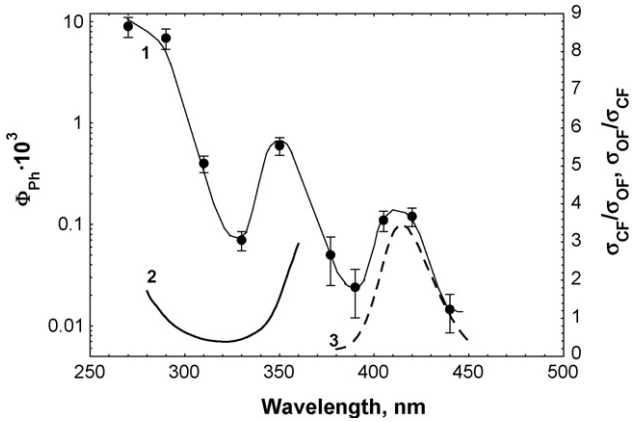

Fig. 7. Spectral dependences of the photodecomposition quantum yield Φ_{Ph} (λ) of **1** in (1) hexane, (2) the ratio of the absorption cross-sections σ_{CF}/σ_{OF} and (3) σ_{OF}/σ_{CF}. The solid line in (1) is presented as a guide.

the most efficient excitation wavelengths for the irradiation dose, $F \leq 10^{17}$ photon cm^{-2}, with maximum efficiency at 330 nm. Irradiation conditions in which $F \geq 5 \times 10^{17}$ photon cm^{-2} corresponded to the most effective writing wavelengths at λ_{exc} ≈320–325 and ≈410–420 nm, with maximum efficiency at the peak of long wavelength absorption band. All calculated processes corresponded to linear excitation, i.e. were independent of light irradiance.

3.4. Photochemical stability

Photodecomposition quantum yields of **1**, Φ_{Ph}, were determined in air-saturated hexane solution at room temperature under steady-state irradiation over a broad spectral range (Fig. 7, curve 1). As can be seen, there was a strong spectral dependence of Φ_{Ph}. The values of $\Phi_{Ph} \ll \{\Phi_{C\rightarrow O}, \Phi_{O\rightarrow C}\}$ revealed slow photochemical processes (velocity constants ~10^8–10^9 s^{-1}) relative to the fast photochromic transformation (~10^{11}–10^{12} s^{-1}) [20], i.e. photodecomposition of **1** proceeds under the constant equilibrium between two forms. The excited states of the O- and C-forms undergo photodecomposition simultaneously. It is difficult to separate quantitatively, the quantum yields of these processes in the 270–440 nm spectral range from the experimental values of Φ_{Ph}, due to unknown lifetimes of the excited states of **1**.

The kinetic analysis of the possible photodecomposition processes was performed for the equilibrium state of **1** for different excitation wavelengths and reaction pathways. From this analysis, the value of Φ_{Ph} should be independent of the absorption cross-sections σ_{OF} and σ_{CF}, in the case of the first-order photochemical reactions proceeding from the lowest electronic excited state of the O- and C-forms. Nevertheless, the experimentally observed spectral dependence of Φ_{Ph} (Fig. 7, curve 1) was strong and exhibited two peaks at λ_{exc} ≈350 and ≈410 nm. The spectral behavior of Φ_{Ph} was similar to the corresponding dependence of the ratio, σ_{CF}/σ_{OF} in the range $\lambda_{exc} \leq 350$ nm (curve 2), and to the reverse ratio σ_{OF}/σ_{CF}, at $\lambda_{exc} \geq 390$ nm. This suggests relatively complex photochemical reactions simultaneously proceed from different excited electronic states of the O- and C-forms and cannot be described by first-order photoreactions.

From the data in Fig. 7, one can see the highest photochemical stability of **1** in hexane corresponded to the excitation wavelengths λ_{exc} ≈390 and ≈440 nm ($\Phi_{Ph} \sim (1.5–2) \times 10^{-5}$), which can be used for optimization of the writing process with increased value of the fatigue resistance.

3.5. Photochromic transformation under two-photon excitation

The 2PA spectrum of the O-form of **1** is shown in Fig. 8 (curve 2). The maximum of the 2PA spectrum ($\lambda_{exc} = 674$ nm) corresponded to $\lambda_{max} = 337$ nm, with the 2PA cross-section ≈80 GM being relatively large compared to other diarylethene derivatives, e.g., for B1536 the reported value was <1 GM [26], and, thus, promising for practical applications. According to quantum–chemical calculations, the observed 2PA band corresponded to the $S_0 \rightarrow S_2$ two-photon allowed transition in the O-form (Table 1). It can be assumed that the shoulder in the 2PA spectrum at ≈405 nm is due to the long wavelength, lower energy transition in the O-form, $S_0 \rightarrow S_1$.

Evidence of the two-photon induced photochromic cyclization reaction O → C of **1** under picosecond irradiation is shown in Fig. 9. The changes in the absorption spectrum of the O-form during irradiation were sufficiently small ($D < 0.03$), ensuring that no reverse reactions occurred in the excitation volume, i.e. the concentration of the C-form in the solution was negligible. In this case the quantum yield of the cyclization reaction of **1** under two-photon excitation, $\Phi_{2PA}^{O\rightarrow C}$, can be estimated using 2PA spectrum of the O-form (Fig. 8, curve 2) and a Gaussian spatial and temporal beam profile approximation. The value of $\Phi_{2PA}^{O\rightarrow C} \approx 0.22 \pm 0.05$ was obtained at $\lambda_{exc} = 810$ nm, comparable to the corresponding one-photon cyclization reaction quantum yield $\Phi_{O\rightarrow C} \approx 0.23 \pm 0.02$ at $\lambda_{exc} = 405$ nm (Fig. 4a, curve 1). Good agreement of these values strongly supports the similar nature of the cyclization process of this diarylethene derivative under one- and two-photon excitation.

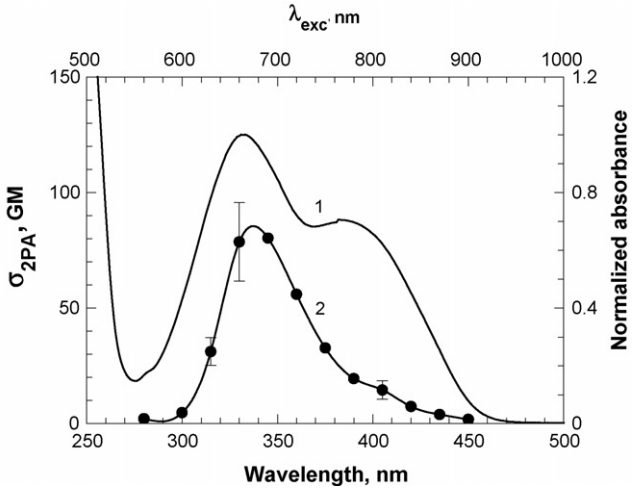

Fig. 8. Normalized (1) linear absorption and (2) 2PA spectra of the O-form of **1** in hexane.

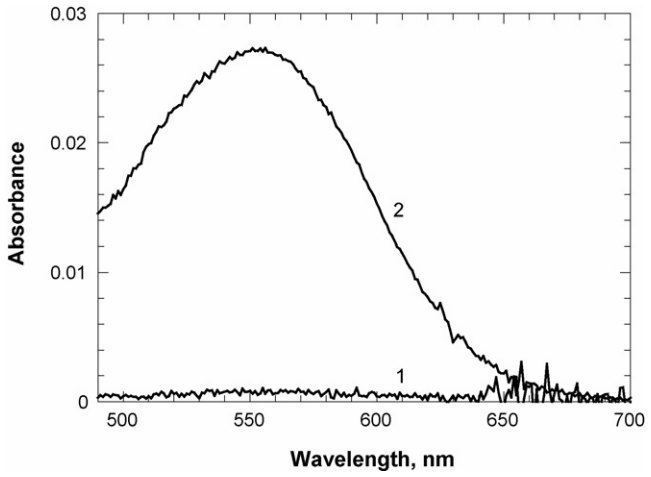

Fig. 9. Absorption spectra of **1** in hexane ($C \approx 4.3 \times 10^{-3}$ M): (1) before and (2) after irradiation for 300 min at $\lambda_{exc} = 810$ nm, with $\tau_p \approx 35$ ps (FWHM), $E_P \approx 25$ μJ and $f = 10$ Hz.

4. Conclusions

The steady-state spectral properties of **1** in hexane, and the results of the quantum–chemical calculations, revealed a relatively complex long wavelength absorption band of the O-form. The broad O-form absorption spectrum corresponded to three strongly overlapped electronic transitions with different orientations of their transition dipoles. The photochromic cyclization and cycloreversion reaction quantum yields, $\Phi_{O\rightarrow C}$ and $\Phi_{C\rightarrow O}$, were determined over a broad spectral range and the optimal writing wavelengths were found for different irradiation doses. The photochemical stability of **1** was investigated in hexane, and corresponding photodecomposition quantum yields, Φ_{Ph}, were determined for different λ_{exc}. The highest photostability under one-photon excitation, $\Phi_{Ph} \approx (1.5\text{–}2) \times 10^{-5}$, was obtained at $\lambda_{exc} \approx 390$ and ≈ 440 nm, useful information to enable optimization of the writing processes.

The 2PA spectrum of the O-form of **1** was obtained with the maximum cross-section ≈80 GM at 674 nm. This corresponded to the transition with λ_{max} of 337 nm. The two-photon induced cyclization reaction of **1** was demonstrated under picosecond excitation at $\lambda_{exc} = 810$ nm. The estimated 2PA photocyclization quantum yield, $\Phi_{2PA}^{O\rightarrow C} \approx 0.22 \pm 0.05$, was in good agreement with the corresponding value of $\Phi_{O\rightarrow C} \approx 0.23 \pm 0.02$ under one-photon excitation, compelling evidence that both one- and two-photon induced cyclization reaction of **1** occurs by similar means.

Acknowledgments

We wish to acknowledge the U.S. Civilian Research and Development Foundation (UK-C2-2574-MO-04), the donors of The Petroleum Research Fund of the American Chemical Society, the National Science Foundation (ECS-0217932 and DMR-9975773) and the University of Central Florida Presidential Initiative for Major Research Equipment for partial support of this work.

References

[1] S. Kawata, Y. Kawata, Chem. Rev. 100 (2000) 1777–1788.
[2] Y. Liang, A.S. Dvornikov, P.M. Rentzepis, Tetrahedron Lett. 40 (1999) 8067–8069.
[3] A. Toriumi, J.M. Herrmann, S. Kawata, Opt. Lett. 22 (1997) 555–557.
[4] B. Chen, M. Wang, C. Li, H. Xia, H. Tian, Synth. Met. 135–136 (2003) 491–492.
[5] Y. Hirshberg, J. Am. Chem. Soc. 78 (1956) 2304–2312.
[6] T. Ikeda, Y. Wu, Pure Appl. Chem. 71 (1999) 2131–2136.
[7] A. Bencini, A. Caneschi, C. Carbonera, A. Dei, D. Gatteschi, R. Righini, C. Sangregorio, J. Van Slageren, J. Mol. Struct. 656 (2003) 141–154.
[8] R.E. Del Sesto, A.M. Arif, J.S. Miller, J. Chem. Soc. Chem. Commun. (2001) 2730–2731.
[9] K. Kaneda, T. Arai, Photochem. Photobiol. Sci. 2 (4) (2003) 402–406.
[10] A. Evenzahay, N.J. Turro, J. Am. Chem. Soc. 120 (1998) 1835–1841.
[11] G. Berkovic, V. Krongauz, V. Weiss, Chem. Rev. 100 (2000) 1741–1753.
[12] Y. Liang, A.S. Dvornikov, P.M. Rentzepis, Macromolecules 35 (2002) 9377–9382.
[13] F. Wei, H. Kun, W. Mei-Xiang, Chin. Phys. 14 (2005) 306–310.
[14] M. Irie, M. Mohri, J. Org. Chem. 53 (1988) 803–808.
[15] M. Irie, Chem. Rev. 100 (2000) 1685–1716.
[16] S.L. Gilat, S.H. Kawai, J.-M. Lehn, J. Chem. Soc. Chem. Commun. (1993) 1439–1446.
[17] G.M. Tsivgoulis, J.-M. Lehn, Angew. Chem. (International Ed.) 34 (1995) 1119–1122.
[18] H.-G. Cho, B.-S. Cheong, Bull. Korean Chem. Soc. 19 (1998) 308–313.
[19] K. Higashiguchi, K. Matsuda, S. Kobatake, T. Yamada, T. Kawai, M. Irie, Bull. Chem. Soc. Jpn. 73 (2000) 2389–2394.
[20] H. Miyasaka, S. Araki, A. Tabata, T. Nobuto, N. Mataga, M. Irie, Chem. Phys. Lett. 230 (1994) 249–254.
[21] E. Kim, J. Park, S.Y. Cho, N. Kim, J.H. Kim, ETRI J. 25 (2003) 253–257.
[22] H. Miyasaka, T. Nobuto, M. Murakami, A. Itaya, N. Tamai, M. Irie, J. Phys. Chem. A 106 (2002) 8096–8102.
[23] M. Irie, K. Sayo, J. Phys. Chem. 96 (1992) 7671–7674.
[24] K. Kasatani, T. Fujiwaki, ITE Lett. Batteries, New Technol. Med. 2 (2001) 215–219.
[25] K. Kasatani, S. Kambe, M. Irie, J. Photochem. Photobiol. A: Chem. 122 (1999) 11–15.
[26] Z. Sekkat, H. Ishitobi, S. Kawata, Opt. Commun. 222 (2003) 269–276.
[27] A. Toriumi, S. Kawata, M. Gu, Opt. Lett. 23 (1998) 1924–1926.
[28] M. Gu, J.O. Amistoso, A. Toriumi, M. Irie, S. Kawata, Appl. Phys. Lett. 79 (2001) 148–150.
[29] J.R. Lakowicz, Principles of Fluorescence Spectroscopy, Kluwer Academic/Plenum, New York, 1999.
[30] C. Xu, W.W. Webb, J. Opt. Soc. Am. B 13 (1996) 481–491.
[31] K.D. Belfield, M.V. Bondar, O.V. Przhonska, K.J. Schafer, J. Photochem. Photobiol. A: Chem. 162 (2004) 569–574.
[32] P.P. Feofilov, Polyarizovannaya Luminescenciya Atomov, Molecyl i Kristallov, Moscow, 1959, pp. 144–147.